

# Ab Initio Group Contribution Method for Activation Energies of Hydrogen Abstraction Reactions

Mark Saeys,<sup>[a, b]</sup> Marie-Françoise Reyniers,<sup>[a]</sup> Veronique Van Speybroeck,<sup>[c]</sup> Michel Waroquier,<sup>[c]</sup> and Guy B. Marin<sup>\*[a]</sup>

*The group contribution method for activation energies is applied to hydrogen abstraction reactions. To this end an ab initio database was constructed, which consisted of activation energies calculated with the ab initio CBS-QB3 method for a limited set of well-chosen homologous reactions. CBS-QB3 is shown to predict reaction rate coefficients within a factor of 2–4 and Arrhenius activation energies within 3–5 kJ mol<sup>-1</sup> of experimental data. Activation energies in the set of homologous reactions vary over 156 kJ mol<sup>-1</sup> with the structure of the abstracting radical and over 94 kJ mol<sup>-1</sup> with the structure of the abstracted hydrocarbon. The parameters required for the group contribution method, the so-called standard activation group additivity values, were determined from this database. To test the accuracy of the group*

*contribution method, a large set of 88 additional activation energies were calculated from first principles and compared with the predictions from the group contribution method. It was found that the group contribution method yields accurate activation energies for hydrogen-transfer reactions between hydrogen molecules, alkyl hydrocarbons, and vinylic hydrocarbons, with the largest deviations being less than 6 kJ mol<sup>-1</sup>. For reactions between allylic and propargylic hydrocarbons, the transition state is believed to be stabilized by resonance effects, thus requiring the introduction of an appropriate correction term to obtain a reliable prediction of the activation energy for this subclass of hydrogen abstraction reactions.*

## 1. Introduction

Hydrocarbon radical reactions are key steps in many important chemical transformations, for example, during combustion, polymerization, polymer degradation, and steam cracking of hydrocarbons. Fundamental kinetic models for these processes often involve an extensive network of elementary reactions. The large number of hydrocarbon radical reactions can be organized into a limited number of families. The most important are: i) carbon–carbon and carbon–hydrogen bond scissions and the reverse radical–radical recombinations, ii) hydrogen abstraction reactions, and iii) radical addition to olefins and the reverse  $\beta$  scission of radicals. Building a reaction network for complex radical chemistry is a challenging task and computer algorithms for the automatic generation of complex reaction networks have been developed by various research groups.<sup>[1]</sup> These reaction networks in turn require a large number of kinetic and thermodynamic parameters.

It is nearly impossible to determine the kinetic and thermodynamic parameters for every elementary reaction in the fundamental kinetic model directly from experiment or through the regression of experimental data,<sup>[1a]</sup> and an alternative approach is desirable. We have previously tested the applicability and reliability of ab initio methods for the calculation of activation energies and standard enthalpies of formation of hydrocarbon molecules and radicals.<sup>[2]</sup> It was found that for standard enthalpies of formation, an accuracy of 2.5 kJ mol<sup>-1</sup> can be ob-

tained with the atom-additivity-corrected CBS-QB3 method.<sup>[2]</sup> Herein, we use the selected CBS-QB3 ab initio method to obtain activation energies for the family of hydrogen abstraction reactions. To further illustrate the accuracy of this method, ab initio reaction rate coefficients for selected hydrogen abstraction reactions will be compared to experimental data.

Despite the increasing computational power, it is neither possible nor desirable to calculate all required kinetic parameters from first principles. Therefore, a group contribution method for activation energies was developed which allows the activation energies for all reactions within a family to be obtained by using parameters derived from a limited set of

[a] Prof. M. Saeys, Prof. M.-F. Reyniers, Prof. G. B. Marin  
Laboratorium voor Petrochemische Techniek, Ghent University  
Krijgslaan 281(S5), 9000 Gent (Belgium)  
Fax: (+32) 9-264-49-99  
E-mail: Guy.Marin@Ugent.be

[b] Prof. M. Saeys  
Department of Chemical and Biomolecular Engineering  
National University of Singapore, 4 Engineering Drive 4  
Singapore 117576 (Singapore)

[c] Dr. V. Van Speybroeck, Prof. M. Waroquier  
Center for Molecular Modeling, Laboratory of Theoretical Physics  
Ghent University, Proeftuinstraat 86, 9000 Gent (Belgium)

Supporting information for this article is available on the WWW under <http://www.chemphyschem.org> or from the author.

high-level ab initio calculations.<sup>[3]</sup> This method is a consistent extension of Benson's group additivity method for standard enthalpies of formation.<sup>[4]</sup> In the group contribution method, the activation energy for any reaction within a family is obtained by combining the activation energy of a chosen reference reaction with a perturbation term that depends on structural differences between the transition-state structure of the reference reaction and the transition-state structure of the reaction under study. Its reliability was previously validated for radical addition and  $\beta$  scission reactions.<sup>[3]</sup> Herein, the required parameters, the so-called standard activation group additivity values, are determined for the family of hydrogen abstraction reactions and the validity of the group contribution method for this family is tested for a large set of hydrogen abstraction reactions.

Hydrogen abstraction reactions are among the most studied radical reactions, since they are conceptually simple and yet play a critical role in various chemical and biochemical processes. Detailed theoretical and experimental studies have addressed the  $\text{H}_2 + \text{H}^\cdot$  and the  $\text{CH}_4 + \text{H}^\cdot$  reactions.<sup>[5–14]</sup> In addition, the reactions of the vinyl radical ( $\text{C}_2\text{H}_3^\cdot$ ) with  $\text{H}_2$ ,<sup>[7,15]</sup> the ethynyl radical ( $\text{C}_2\text{H}^\cdot$ ) with  $\text{H}_2$ ,<sup>[16,17]</sup> and the phenyl radical ( $\text{C}_6\text{H}_5^\cdot$ ) with  $\text{H}_2$  and  $\text{CH}_4$ <sup>[18,19]</sup> have been studied theoretically. Hydrogen abstraction reactions are also widely used as benchmarks for the development and testing of new quantum chemical methods.<sup>[8,12,20–23]</sup> Shaik et al.,<sup>[24]</sup> Anderson et al.,<sup>[25]</sup> Zavitsas,<sup>[26]</sup> Ma and Schober,<sup>[27]</sup> and Blowers and Masel<sup>[28]</sup> have developed conceptual frameworks, often based on generalized valence bond theory, to understand reactivity patterns for this family of reactions. Although these models vary in the relative importance they give to different effects, important correlations have been established with the bond energies and the reaction enthalpy, with steric effects, and also in some cases with polar effects, related to charge polarization in the transition state.

The principal aim of this paper is to present a database of high-level ab initio activation energies for a series of well-chosen hydrogen abstraction reactions, and to determine the standard activation group additivity values for the group contribution method for activation energies from first principles. Work is in progress to derive predictive methods for pre-exponential factors, partition functions, and tunneling factors. In Section 2, the computational methods are discussed and the group contribution method is briefly introduced. In Section 3, we illustrate the accuracy of the ab initio CBS-QB3 predicted reaction rate coefficients by comparison with literature data. Next, our database of ab initio activation energies is presented and the standard activation group additivity values are derived. Also in Section 3 the accuracy of the group contribution method is assessed. To better understand the factors governing the reactivity and to test the correlation between activation energies and reaction enthalpies, the model of Blowers and Masel<sup>[28]</sup> is used to analyze the ab initio data. The conclusions of this work are presented in Section 4.

## 2. Methods

### 2.1. Computational Methods

Reaction rate coefficients for bimolecular reactions can be calculated using the microscopic formulation of transition-state theory<sup>e.g.[29]</sup> [Eq. (1)]:

$$k(T) = \kappa(T) \frac{k_B T}{h} \frac{Q_{\text{TS}}(T)}{Q_A(T)Q_B(T)} \exp\left(\frac{-\Delta E^\ddagger(0\text{K})}{RT}\right) \quad (1)$$

in which  $\kappa(T)$  is the tunneling correction factor,  $k_B$  the Boltzmann constant, and  $h$  the Planck constant.  $Q_x(T)$  stands for the partition function evaluated at temperature  $T$ , and  $\Delta E^\ddagger(0\text{K})$  is the energy difference between the reactants and the transition state, including the zero-point energy difference. The translational partition functions are evaluated per unit volume [ $\text{m}^{-3}$ ].

The tunneling correction factor  $\kappa(T)$  was calculated using the one-dimensional Eckart tunneling model.<sup>[30]</sup> The Eckart method is one of the more accurate approximate one-dimensional tunneling corrections.<sup>[31]</sup> The tunneling factor is calculated by fitting an Eckart potential to the minimum energy path using the curvature at the transition state, the energy barrier, and the reaction energy. The transmission probability and  $\kappa(T)$  are then obtained using standard expressions.<sup>[31]</sup> Partition functions  $Q_x(T)$  were calculated using standard thermodynamic formulas.<sup>[29]</sup> For the computation of accurate partition functions, particular attention to internal rotations is required.<sup>[7,32,33]</sup> Here, the one-dimensional hindered rotor approximation is applied. The program developed by Sumathi and Green<sup>[7]</sup> was used to calculate the hindered rotor partition functions. The hindered rotor potential was calculated at the B3LYP/6-311G(d,p) level of theory as a function of the torsional angle in steps of  $10^\circ$ .

Activation energies,  $\Delta E^\ddagger(0\text{K})$ , were computed with the complete basis set CBS-QB3 method of Petersson et al.<sup>[34,35]</sup> The complete basis set family of methods exploits the asymptotic convergence of the pair natural orbital expansions to extrapolate the energy to the second-order Møller–Plesset (MP2) basis set limit. Higher-order contributions to the correlation energy are evaluated with smaller basis sets. Through the introduction of an interference factor derived from generalized valence bond theory arguments,<sup>[35]</sup> an extrapolation to the full configuration interaction/complete basis set level is attempted. The most recent version of the CBS-QB3 method was used,<sup>[34]</sup> where geometry optimization and frequency calculation are done at the B3LYP/6-311G(d,p) level and the higher-order contributions are obtained from MP4(SDQ)/6-31 + G(d,p) and CCSD(T)/6-31 + G(d') computations.

The reliability of the CBS-QB3 method for the computation of thermodynamic and kinetic data for hydrocarbon radical reactions was assessed previously.<sup>[2,8]</sup> It was found that the atom-additivity-corrected CBS-QB3 method yields accurate standard enthalpies of formation with a mean absolute deviation (MAD) of  $2.5\text{ kJ mol}^{-1}$  over a test set of 58 hydrocarbon molecules and radicals ranging from  $\text{C}_1$  to  $\text{C}_{10}$ .<sup>[2]</sup> The accuracy of the B3LYP/6-311G(d,p) method was assessed for transition-state geometries.<sup>[2]</sup> This method is used for geometry optimizations in

CBS-QB3. It was found that for transition states of hydrogen abstraction reactions, B3LYP/6-311G(d,p) geometries show good agreement with geometries from higher-level benchmark calculations. All calculations were performed with the Gaussian 98 computational package.<sup>[36]</sup>

The three fundamental components of the reaction rate expression [Eq. (1)] are the tunneling factor  $\kappa(T)$ , the partition functions  $Q_x(T)$ , and the activation barrier at 0 K,  $\Delta E^\ddagger(0\text{ K})$ . Herein, we will focus on the activation energies,  $\Delta E^\ddagger(0\text{ K})$ , and develop a group contribution scheme for the activation energies. Methods for the accurate prediction of partition functions will be developed separately. Although Arrhenius activation energies do not appear in the microscopic reaction rate expression [Eq. (1)], they will be presented here because of their common use in kinetic studies. If tunneling is neglected, Arrhenius activation energies can be obtained from<sup>[29]</sup> [Eq. (2)]:

$$E_a(T) = \Delta H^\ddagger(T) + (1 - \Delta n^\ddagger)RT \quad (2)$$

where  $\Delta n^\ddagger$  is the change in the number of molecules in going from the reactant to the transition state, that is,  $\Delta n^\ddagger = 0$  for unimolecular reactions and  $\Delta n^\ddagger = -1$  for bimolecular reactions such as hydrogen abstractions.  $\Delta H^\ddagger(T)$ , the enthalpy difference between the transition-state structure and the reactants at temperature  $T$ , is obtained from the CBS-QB3 ab initio calculations. The  $RT$  term and the temperature dependence of  $\Delta H^\ddagger(T)$  make the Arrhenius activation energy temperature dependent, and Arrhenius activation energies at 298 and 1000 K will be reported. Except for the reaction rate coefficient calculations in Section 3.1, the thermal corrections to  $\Delta H^\ddagger(T)$  were calculated with the simple harmonic oscillator approximation and neglecting tunneling. As will be shown in Section 3.1, this can lead to an overestimation of the Arrhenius activation energies by 5–10 kJ mol<sup>-1</sup> at 1000 K and by up to 20 kJ mol<sup>-1</sup> at 298 K.

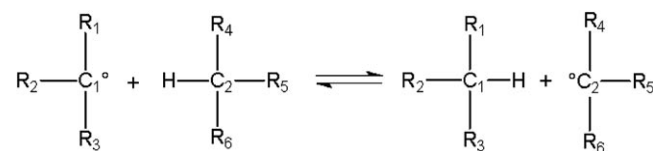
## 2.2. Group Contribution Method for Activation Energies

The group contribution method for activation energies<sup>[3]</sup> is a consistent extension of Benson's group additivity method<sup>[4]</sup> for standard enthalpies of formation of stable species. This method allows activation energies to be calculated for all reactions within a given family based on a limited number of parameters. In Benson's method, a group is defined as "a polyvalent atom (ligancy  $\geq 2$ ) in a molecule together with all its ligands".<sup>[4]</sup> A group is characterized as X-(A)<sub>i</sub>(B)<sub>j</sub>(C)<sub>k</sub>(D)<sub>l</sub>, where X is the polyvalent central atom, attached to  $i$  A atoms,  $j$  B atoms, etc. For hydrocarbons the central atom X is a carbon atom. Different types of carbon atoms are distinguished: C<sub>d</sub> stands for a double- and C<sub>t</sub> for a triple-bound carbon atom, C<sup>•</sup> stands for a radical carbon center, and C<sub>B</sub> for a carbon atom in a benzene ring. For every group a contribution to the standard enthalpy of formation of a molecule is defined in Benson's method. Additional contributions for non-nearest-neighbor interactions, such as *gauche*-, *cis*-, or 1,5-interactions, are also included. All of the above contributions are called group additivity values (GAVs). The standard enthalpy of formation of a molecule is then written as a sum of GAVs [Eq. (3)]:

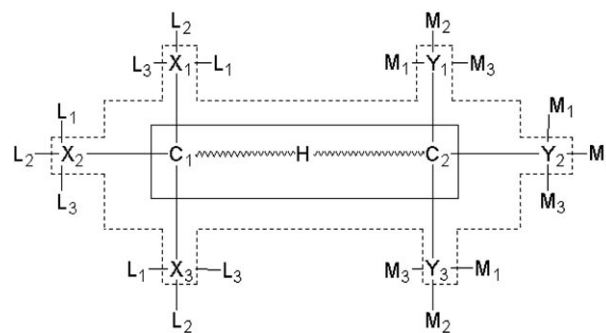
$$\Delta_f H^\circ = \sum_i \text{GAV}(C_i) + \sum_j \text{GAV}(\text{NNN}_j) \quad (3)$$

where  $\text{GAV}(C_i)$  is the group additivity value for the group with  $C_i$  as central atom, and  $\text{GAV}(\text{NNN}_j)$  is a group additivity value for a non-nearest-neighbor interaction.

Formally, the standard enthalpy of formation of a transition state can be expressed in a similar way. A schematic representation of a hydrogen abstraction reaction and the corresponding transition state are shown in Figures 1 and 2. It should be



**Figure 1.** Schematic representation of a hydrogen abstraction reaction. R<sub>i</sub> indicate alkyl substituents.



**Figure 2.** Schematic representation of the transition state of a hydrogen abstraction. The central atoms of the primary groups are enclosed by the full line. The delimitation of the reactive moiety depends on the degree to which neighbor effects are taken into account. The dotted line corresponds to the reactive moiety if next-nearest-neighbor effects can be neglected.

stressed that in the transition state the two carbon atoms  $C_1$  and  $C_2$ , which play a central role in the reactive moiety, may not be classified in the five above-mentioned types of carbon atoms, that is, C, C<sup>•</sup>, C<sub>d</sub>, C<sub>t</sub>, or C<sub>B</sub>. Therefore, new, transition-state-specific types of carbon atom need to be introduced:  $C_1^{\text{TS}}$  and  $C_2^{\text{TS}}$ . This leads to three categories of transition-state-specific GAVs (Figure 2): i) *primary* GAVs for groups where  $C_i^{\text{TS}}$  is a central atom:  $C_1^{\text{TS}}-(X_1)(X_2)(X_3)$  and  $C_2^{\text{TS}}-(Y_1)(Y_2)(Y_3)$ ; ii) *secondary* GAVs for groups where  $C_i^{\text{TS}}$  is a ligand atom:  $X_i-(C_1^{\text{TS}})(L_1)(L_2)(L_3)$  and  $Y_i-(C_2^{\text{TS}})(M_1)(M_2)(M_3)$ ; and iii) *tertiary* GAVs for nonnearest-neighbor interactions involving  $C_1^{\text{TS}}$  and/or  $C_2^{\text{TS}}$ , that is, for interactions between  $X_i$  and  $Y_j$ , or for modified interactions between  $Y_1$  and  $M_j$  on  $Y_2$  or  $Y_3$ , etc. Groups further away from the reactive moiety  $C_1^{\text{TS}}\cdots\text{H}\cdots\text{C}_2^{\text{TS}}$  do not include transition-state-specific atom types and are therefore identical to corresponding groups in the reactants: they are non-transition-state-specific groups.

In the transition state the transferred H atom is, in principle, also a polyvalent atom (ligancy = 2) and thus would require

transition-state-specific GAVs. However, in the reactants, the transferred H atom,  $\cdots\text{H}\cdots$ , is associated to the  $\text{C}_2$  group (Figure 1). Analogously, in the transition state the  $\cdots\text{H}\cdots$  atom can be included in the  $\text{C}_2^{\text{TS}}$  group by definition. The standard enthalpy of formation of the transition state can now be expressed as [Eq. (4)]:

$$\Delta_r H^\circ(\text{TS}) = \underbrace{\sum_{i=1}^2 \text{GAV}(\text{C}_i^{\text{TS}})}_{\text{primary GAVs}} + \underbrace{\sum_{k=1}^3 \text{GAV}(\text{X}_k) + \sum_{l=1}^3 \text{GAV}(\text{Y}_l)}_{\text{secondary GAVs}} + \underbrace{\sum_j \text{GAV}(\text{NNN}_j)}_{\text{tertiary GAVs}} + \underbrace{\sum \text{GAV}}_{\text{non-TS-specific}} \quad (4)$$

The activation energy is determined by the difference between the enthalpy of formation of the transition state and the enthalpy of formation of the reactants. It can therefore be expressed as a sum of  $\Delta\text{GAV}$ s, the so-called activation group additivity values (Eqs. (2)–(4) and Figure 2) [Eq. (5)]:

$$E_a(T) = \underbrace{\sum_{i=1}^2 \Delta\text{GAV}(\text{C}_i)}_{\text{primary}} + \underbrace{\sum_{k=1}^3 \Delta\text{GAV}(\text{X}_k) + \sum_{l=1}^3 \Delta\text{GAV}(\text{Y}_l)}_{\text{secondary}} + \underbrace{\sum_j \Delta\text{GAV}(\text{NNN}_j)}_{\text{tertiary}} + 2RT \quad (5)$$

where [Eq. (6)]

$$\Delta\text{GAV} = \text{GAV}(\text{TS}) - \text{GAV}(\text{Reactant}) \quad (6)$$

Only  $\Delta\text{GAV}$ s for transition-state-specific groups remain in the expression, as the non-transition-state-specific GAVs cancel. The primary and secondary activation group additivity values,  $\Delta\text{GAV}$ , are determined by the difference in GAVs of groups that differ in only one atom: for example,  $\text{C}_1\text{-(C)}(\text{H})_3$  and  $\text{C}_1^{\text{TS}}\text{-(C)}(\text{H})_3$ , or  $\text{C-(C}_2\text{)}(\text{C)}(\text{H})_2$  and  $\text{C-(C}_2^{\text{TS}}\text{)}(\text{C)}(\text{H})_2$ . The magnitude of the  $\Delta\text{GAV}$ s can be estimated from the variation of the GAVs of stable molecules. GAVs vary strongly with the carbon type of the central atom: for example,  $\text{C-(C)}(\text{H})_3$  amounts to  $-41.8 \text{ kJ mol}^{-1}$ , whereas  $\text{C}^{\cdot}\text{-(C)}(\text{H})_2$  is  $171.5 \text{ kJ mol}^{-1}$ .<sup>[4]</sup> Therefore the primary  $\Delta\text{GAV}$ s can be expected to be large. GAVs vary much less with the carbon type of the ligand atom: for example,  $\text{C-(C}_2\text{)}(\text{H})_2$  is  $-20.9 \text{ kJ mol}^{-1}$  and  $\text{C-(C}^{\cdot}\text{)}(\text{C)}(\text{H})_2$  is  $-20.6 \text{ kJ mol}^{-1}$ .<sup>[4]</sup> The secondary  $\Delta\text{GAV}$ s can thus be expected to be small. GAVs for non-nearest-neighbor interactions are in general small, typically 3 to  $5 \text{ kJ mol}^{-1}$ <sup>[4]</sup> and the tertiary  $\Delta\text{GAV}$ s can also be expected to be small. The main contribution to the activation energy will therefore come from the primary activation group additivity values,  $\Delta\text{GAV}(\text{C})$ . Calculations did indeed confirm that secondary and tertiary effects on the activation energy can be neglected to a good approximation for reactions involving hydrocarbon radicals (see the Supporting Information).

Equation (5) can be made more accessible for applications by introducing a reference or standard reaction. The activation

energy of the reaction under study is then written as the activation energy of the reference reaction plus perturbation terms that take into account the structural differences between the reference reaction and the studied reaction [Eq. (7)]:

$$E_a(T) = E_{a,\text{Ref}}(T) + \underbrace{\sum_{i=1}^2 \Delta\text{GAV}^\circ(\text{C}_i)}_{\text{primary}} + \underbrace{\sum_{i=1}^3 \Delta\text{GAV}^\circ(\text{X}_i) + \sum_{i=1}^3 \Delta\text{GAV}^\circ(\text{Y}_i)}_{\text{secondary}} + \underbrace{\sum_j \Delta\text{GAV}^\circ(\text{NNN}_j)}_{\text{tertiary}} \quad (7)$$

This alternative formulation corresponds to a shift of the reference point for the activation energies from  $0 \text{ kJ mol}^{-1}$  in Equation (5) to  $E_{a,\text{Ref}}$  in Equation (7).

An advantage of this formulation is that the leading term of the activation energy, given by the reference reaction, is separated from the perturbation. Since ab initio calculations yield more accurate relative than absolute data,<sup>[14,20,37]</sup> the perturbation terms,  $\Delta\text{GAV}^\circ$ , can be expected to be more accurate than the leading  $E_{a,\text{Ref}}$  term. In principle then, the accuracy of the group contribution method can be further enhanced by obtaining the activation energy for the reference reaction from accurate experimental data or from very high-level ab initio methods. A second advantage is that most of the temperature effect on the Arrhenius activation energies  $E_a(T)$  will be taken into account through the reference activation energy,  $E_{a,\text{Ref}}(T)$ , and hence the standard activation group additivity values,  $\Delta\text{GAV}^\circ$ s, are much less temperature dependent than the  $\Delta\text{GAV}$ s in Equation (5). As stated, the focus of this paper will be on the more fundamental activation barrier at 0 K,  $\Delta E^\ddagger(0 \text{ K})$ , and the standard activation group additivity values,  $\Delta\text{GAV}^\circ$ , will be derived for the barrier at 0 K. However, the reported  $\Delta\text{GAV}^\circ$ s can be expected to be rather accurate for Arrhenius activation energies at different temperatures as well, since the main temperature effect is absorbed into the reference activation energy and the latter will be significantly temperature dependent.

The validity of Equations (5) and (7) depends on the validity of the group additivity method for the standard enthalpy of formation of the transition state [Eq. (4)]. Recently, Sumathi et al.<sup>[7c]</sup> discussed this point for hydrogen abstraction reactions and gave a qualitative justification for the group concept using an atoms-in-molecules<sup>[38]</sup> analysis. In this work the validity of the group concept is tested by comparing results from the group contribution method with ab initio CBS-QB3 activation energies,  $\Delta E^\ddagger(0 \text{ K})$ . Clearly, direct comparison of the theoretical activation energies with experimental data would be preferable. However, as discussed in our previous paper,<sup>[2]</sup> experimental Arrhenius activation energies are not available for most of the reactions studied. Moreover, as illustrated in Section 3.1, the available experimental activation energies show large discrepancies among each other, which hampers a direct comparison with the theoretical predictions. Indeed, most experimental studies report reaction rate coefficients, or the de-

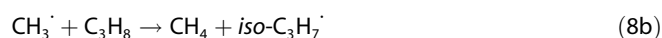
rived Arrhenius activation energies, rather than the more fundamental  $\Delta E^\ddagger(0\text{ K})$ .

### 3. Results and Discussion

In this section, a database of accurate ab initio activation energies for a large set of homologous hydrogen abstraction reactions, including primary, secondary, and tertiary alkyl, allylic, vinylic, naphthenic, benzylic, and propargylic radicals, is constructed. The goal is to determine the standard activation group additivity values,  $\Delta\text{GAV}^\circ$  [Eq. (7)], for the dominant primary groups from the ab initio database. The accuracy of the ab initio predicted reaction rate coefficients is illustrated in Section 3.2. Next, the primary standard activation group additivity values are derived and the importance of the secondary standard activation group additivity values is discussed. In the last section the group contribution method is validated by comparison with a large set of ab initio CBS-QB3 activation energies for reactions not included in the ab initio database.

#### 3.1. Assessment of the Ab Initio Reaction Rate Coefficients

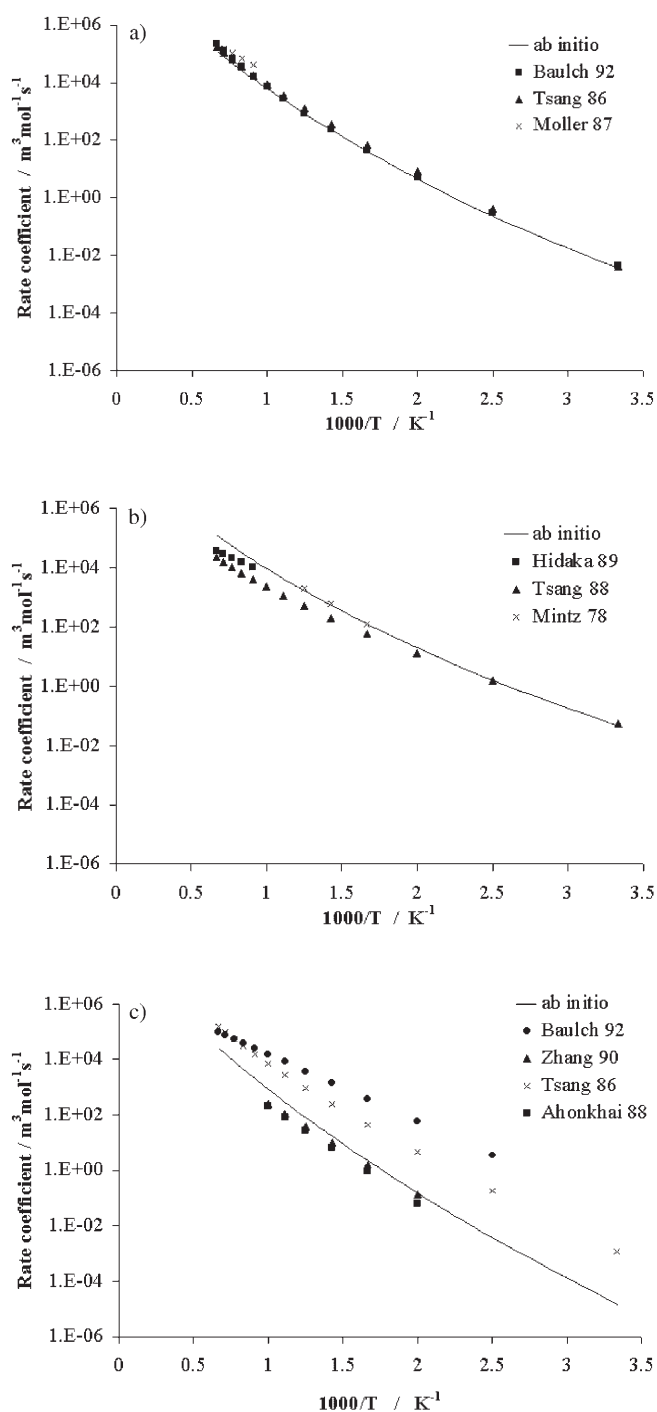
To illustrate the accuracy of the selected CBS-QB3 ab initio method, reaction rate coefficients were calculated for three well-studied hydrogen abstraction reactions [Eqs. (8a), (8b), and (8c)]:



and compared with experimental reaction rate coefficients obtained from the NIST chemical kinetics database.<sup>[39]</sup>

Arrhenius diagrams of the predicted reaction rate coefficients, calculated using Equation (1), are plotted in Figure 3, together with available experimental data. Table 1 gives an overview of the calculated activation energies using different levels of theory, and compares the predicted values with experimental Arrhenius activation energies. Note that reaction rates are measured experimentally, and that the Arrhenius activation energies are derived parameters. As a result, important differences between the reported experimental Arrhenius activation energies can be found (Table 1), although the reported experimental reaction rate coefficients agree fairly well (Figure 3).

For the well-studied reaction (8a), see Figure 3a, very good agreement between the experimental and ab initio reaction rate coefficients is found over the entire temperature range of 300–1500 K. The good agreement is reflected by the Arrhenius activation energies (Table 1). At 298 K, the ab initio activation energy seems slightly low, possibly because the large effect of tunneling on the activation energy is slightly overestimated by the approximate one-dimensional Eckart model based on a fitted potential. Correctly treating the internal rotations as hindered rotors instead of harmonic oscillators lowers the calcu-



**Figure 3.** Comparison of ab initio CBS-QB3 predicted rates with literature data from the NIST chemical kinetics database.<sup>[39]</sup> a) Hydrogen abstraction from ethane by a methyl radical. b) Abstraction of a secondary hydrogen atom from propane by a methyl radical. c) Hydrogen abstraction from ethene by a methyl radical.

lated activation energies, especially at higher temperatures. Tunneling effects are most important at lower temperatures and lower the calculated Arrhenius activation energies by  $23\text{ kJ mol}^{-1}$  at 298 K. The combination of hindered rotor partition functions and Eckart tunneling lowers the calculated Arrhenius activation energies by about  $24\text{ kJ mol}^{-1}$  at 298 K and by about  $9\text{ kJ mol}^{-1}$  at 1000 K.

**Table 1.** Overview of ab initio CBS-QB3 and experimental<sup>[39]</sup> activation energies. Influence of the level of theory and of the temperature.

	$\Delta E^\ddagger(0\text{ K})$ ab initio	Arrhenius $E_a$ (298 K)				Arrhenius $E_a$ (1000 K)			
		HO <sup>[a]</sup>	HR <sup>[a]</sup>	HR+T <sup>[a]</sup>	Experimental	HO <sup>[a]</sup>	HR <sup>[a]</sup>	HR+T <sup>[a]</sup>	Experimental
$\text{CH}_3^\cdot + \text{C}_2\text{H}_6 \rightarrow \text{CH}_4 + \text{C}_2\text{H}_5^\cdot$	58.9	60.3	59.1	35.9	40.2; <sup>[b]</sup> 44.6 <sup>[c]</sup>	78.4	73.6	69.5	56.5; <sup>[d]</sup> 68.0; <sup>[c]</sup> 75.2 <sup>[b]</sup>
$\text{CH}_3^\cdot + \text{C}_3\text{H}_8 \rightarrow \text{CH}_4 + \text{iso-C}_3\text{H}_7^\cdot$	48.5	50.5	49.6	29.3	31.5 <sup>[e]</sup>	68.8	63.9	60.2	43.1; <sup>[f]</sup> 51.7; <sup>[e]</sup> 55.5 <sup>[g]</sup>
$\text{CH}_3^\cdot + \text{C}_2\text{H}_4 \rightarrow \text{CH}_4 + \text{C}_2\text{H}_3^\cdot$	69.3	70.7	69.6	50.7	49.0 <sup>[c]</sup>	88.7	84.8	80.9	46.6; <sup>[h]</sup> 63.0; <sup>[i]</sup> 70.6; <sup>[c]</sup> 71.6 <sup>[j]</sup>

[a] HO: harmonic oscillator approximation; HR: hindered rotor approximation without tunneling; HR+T: hindered rotor approximation with Eckhart tunneling. [b] Ref. [44] (experimental temperature range: 300–1500 K). [c] Ref. [43] (300–2500 K). [d] Ref. [47] (1100–1400 K). [e] Ref. [41] (300–2500 K). [f] Ref. [48] (1100–1145 K). [g] Ref. [40] (609–648 K). [h] Ref. [44] (400–3000 K). [i] Ref. [42] (650–770 K). [j] Ref. [39] (673–766 K).

For reaction (8b), fair agreement is observed for the reaction rates (Figure 3b), in particular with the direct experimental data of Mintz et al.<sup>[40]</sup> and, at lower temperatures, with the data of Tsang.<sup>[41]</sup> At higher temperatures the ab initio prediction overestimates the reaction rate coefficients put forward in a review article by Tsang.<sup>[41]</sup> The ab initio Arrhenius activation energies in Table 1 are in good agreement with the experimental values. The ab initio activation energy at 650 K ( $50.1\text{ kJ mol}^{-1}$ ) agrees reasonably well with the experimental value of  $55.5\text{ kJ mol}^{-1}$  reported by Mintz et al.<sup>[40]</sup>

For reaction (8c), important differences can be found between the experimental reaction rate coefficients from different studies (Figure 3c). The reaction rate coefficient for this reaction is difficult to measure, because the significantly faster radical addition reaction occurs simultaneously. Indeed, the ab initio barrier for methyl radical addition is  $38\text{ kJ mol}^{-1}$  lower than the ab initio barrier for hydrogen abstraction. Our ab initio rate coefficient agrees with the experimental data from Ahonkai et al.<sup>[39]</sup> and Zhang et al.,<sup>[42]</sup> but is significantly lower than the values presented in reviews by Tsang et al.<sup>[43]</sup> and Baulch et al.<sup>[44]</sup> The slope of the ab initio values, however, agrees rather well with the data from Tsang et al.<sup>[43]</sup> The ab initio activation energy in the 650–700 K range ( $71.1\text{ kJ mol}^{-1}$ ) is comparable to the experimental value of  $71.6\text{ kJ mol}^{-1}$  reported by Ahonkai et al.<sup>[39]</sup>

In general it can be concluded that our ab initio method predicts reaction-rate coefficients within a factor 2 to 4 of experimental data and Arrhenius activation energies within 3–5  $\text{kJ mol}^{-1}$ . A similar observation was made by Sumathi and Green for the analogous CBS-Q method.<sup>[7a]</sup> In a benchmark study on hydrogen abstraction reactions, Coote also found that the CBS-QB3 method can accurately predict abstraction barriers, typically within  $2\text{ kJ mol}^{-1}$  of very high-level W1 ab initio calculations.<sup>[8]</sup> The CBS-QB3 barriers were found to be generally slightly lower than the W1 barriers. Comparison with experimental data, on the other hand, seems to suggest that the CBS-QB3 barriers are slightly high. However, comparison with experimental Arrhenius activation energies remains difficult because of the important uncertainty in the experimental values.



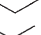

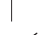



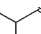

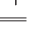



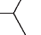

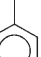









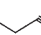

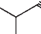





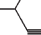



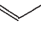



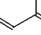

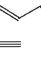



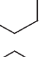



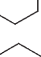

### 3.2. Ab Initio Database of Activation Energies and Determination of the Standard Activation Group Additivity Values

Activation energies were calculated for hydrogen abstraction reactions by methyl radicals at various types of carbon atoms and for the reverse reactions, that is, abstraction of a hydrogen atom from methane by various types of hydrocarbon radicals. This allows quantification of the influence of the structure near the abstracted hydrogen atom ( $\text{C}_2$  in Figure 1) and the influence of the structure of the abstracting radical ( $\text{C}_1$  in Figure 1) on the activation energy. In addition to the fundamental activation barrier at 0 K [ $\Delta E^\ddagger(0\text{ K})$ ], we also report the Arrhenius activation energies at 298 and 1000 K. The focus of the discussion will be on the 0 K barrier.

Particularly relevant to our discussion is the work by Sumathi et al.<sup>[7]</sup> These authors have studied hydrogen abstractions by hydrogen radicals from various alkanes, alkenes, and alkynes, and abstractions by methyl radicals from alkanes. They derived GAVs from modified CBS-Q calculations for the enthalpy of formation of the transition state. Their approach differs from the approach used herein in a number of ways: i) the central concept in their approach is the enthalpy of formation of the transition state, whereas in our approach the activation energy is the central concept; ii) Sumathi et al. combine experimental GAVs for the reactants with theoretical GAVs for the transition state, but in our approach all parameters are derived from first principles, thus leading to a thermodynamically consistent method;<sup>[3]</sup> and iii) the group additivity method of Sumathi et al. introduces so-called supergroups. A supergroup is not a Benson group but encompasses the abstracting radical atom, the transferred hydrogen atom, and the formed radical carbon atom, that is, two Benson-type groups. Our method uses only Benson groups, which allow an order of magnitude reduction of the number of GAVs. Indeed, whereas the approach of Sumathi et al. requires  $C_{29}^2 = 406$  GAVs for 29 types of radicals, our approach requires only  $2 \times 28$   $\Delta\text{GAV}^\circ$ s. Moreover, supergroups are much larger than Benson groups and many supergroup GAVs are too large for high-level ab initio calculations, for example, groups involving combinations of allylic, propargylic, or benzylic species. The large computational cost limited the number of supergroup GAVs reported by Sumathi et al. to 27.

In Table 2, CBS-QB3 activation energies are reported for abstractions by methyl radicals that form 29 different product

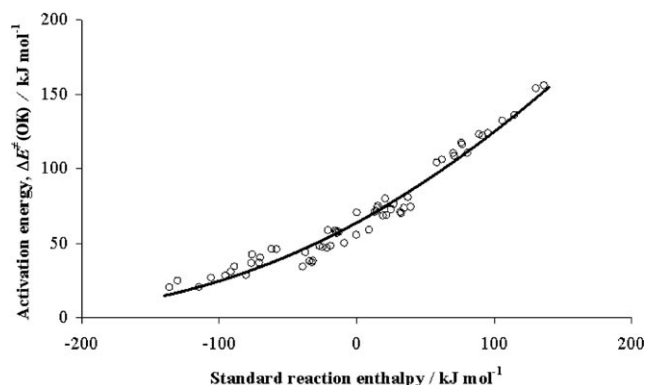
**Table 2.** Ab initio activation energies [kJ mol<sup>-1</sup>] for hydrogen abstraction reactions. Influence of the structure of the abstracting radical and of the abstracted hydrocarbon molecule.

Reaction	Forward			Reverse		
	0 K	298 K	1000 K	0 K	298 K	1000 K
1 Me° + H <sub>2</sub> ⇌ CH <sub>4</sub> + H°	58.8	55.7	63.3	56.0	56.0	66.5
2 Me° + CH <sub>4</sub> ⇌ CH <sub>4</sub> + Me°	71.0	71.0	88.7	71.0	71.0	88.7
3 Me° +  ⇌ CH <sub>4</sub> + 	58.9	60.3	78.4	75.2	75.8	94.2
4 Me° +  ⇌ CH <sub>4</sub> + 	48.5	50.5	68.8	76.7	77.6	96.8
5 Me° +  ⇌ CH <sub>4</sub> + 	38.3	41.1	59.6	73.9	75.5	96.1
6 Me° +  ⇌ CH <sub>4</sub> + 	42.9	44.3	62.2	117.7	120.3	140.0
7 Me° +  ⇌ CH <sub>4</sub> + 	34.8	36.8	55.1	123.4	125.9	145.8
8 Me° +  ⇌ CH <sub>4</sub> + 	28.5	30.8	49.0	124.1	126.3	146.6
9 Me° +  ⇌ CH <sub>4</sub> + 	25.2	27.4	45.9	154.2	157.7	178.3
10 Me° +  ⇌ CH <sub>4</sub> + 	20.7	22.6	40.7	156.2	158.9	179.6
11 Me° +  ⇌ CH <sub>4</sub> + 	46.5	47.7	65.5	106.4	109.5	129.1
12 Me° +  ⇌ CH <sub>4</sub> + 	40.7	42.9	61.1	110.6	113.1	133.0
13 Me° +  ⇌ CH <sub>4</sub> + 	37.0	39.2	57.6	116.6	115.9	134.4
14 Me° +  ⇌ CH <sub>4</sub> + 	46.3	47.4	65.4	104.4	105.7	124.6
15 Me° +  ⇌ CH <sub>4</sub> + 	37.3	39.4	57.6	108.8	110.4	130.0
16 Me° +  ⇌ CH <sub>4</sub> + 	29.0	31.7	50.1	110.7	112.2	132.5
17 Me° +  ⇌ CH <sub>4</sub> + 	27.1	29.3	47.5	132.5	135.2	155.4
18 Me° +  ⇌ CH <sub>4</sub> + 	20.9	23.4	41.8	136.2	138.1	158.8
19 Me° +  ⇌ CH <sub>4</sub> + 	69.3	70.7	88.7	47.2	49.0	68.7
20 Me° +  ⇌ CH <sub>4</sub> + 	59.4	61.5	79.6	50.4	52.6	72.9
21 Me° +  ⇌ CH <sub>4</sub> + 	59.1	61.4	79.4	80.1	82.2	101.4
22 Me° +  ⇌ CH <sub>4</sub> + 	58.0	60.4	78.3	73.9	75.2	94.0
23 Me° +  ⇌ CH <sub>4</sub> + 	48.6	50.6	68.5	69.0 <sup>[a]</sup>	69.7 <sup>[a]</sup>	89.1 <sup>[a]</sup>
24 Me° +  ⇌ CH <sub>4</sub> + 	115.6	120.9	128.9	0.0	0.0	0.0
25 Me° +  ⇌ CH <sub>4</sub> + 	74.5	77.3	95.1	34.7	38.1	59.1
26 Me° +  ⇌ CH <sub>4</sub> + 	47.8	50.4	68.7	73.0	75.3	94.7
27 Me° +  ⇌ CH <sub>4</sub> + 	44.2	45.9	64.0	81.0	83.2	102.4
28 Me° +  ⇌ CH <sub>4</sub> + 	37.5	40.1	58.2	70.5	72.5	93.0
29 Me° +  ⇌ CH <sub>4</sub> + 	31.3	33.6	51.9	122.4	125.2	145.3

[a] CBS-RAD (QCISD,B3LYP).<sup>[45]</sup>

radicals and for the reverse reactions. The activation energies for these two homologous sets of reactions are sufficient to derive all the primary standard group additivity values for hydrogen abstraction reactions.

The activation energies,  $\Delta E^\ddagger(0\text{ K})$ , for the forward reactions vary between 20.7 and 115.6  $\text{kJ mol}^{-1}$ , whereas for the reverse reactions the activation energies lie between 0.0 and 156.2  $\text{kJ mol}^{-1}$ . To understand the factors governing the abstraction barrier, the activation energies from Table 2 are plotted against the standard reaction enthalpies,  $\Delta_r H(298\text{ K})$  (see Figure 4). It is clear that the relative strength of the breaking



**Figure 4.** Evans–Polanyi plot for the hydrogen abstraction reactions from Table 2. The curve corresponds to the model of Blowers and Masei<sup>[28]</sup> [Eq. (10)] with an adjusted value of 64.0  $\text{kJ mol}^{-1}$  for the intrinsic activation energy  $E_a^0$ .

and the forming C–H bond is the determining factor for the activation energy for this set of reactions. However, the trend deviates significantly from a linear Evans–Polanyi-type correlation<sup>[46]</sup> [Eq. (9)]:

$$E_a = E_a^0 + \gamma_p \Delta_r H \quad (9)$$

The curve in Figure 4 was obtained using a model proposed by Blowers and Masei,<sup>[28]</sup> which is a refinement of the Evans–Polanyi model [Eq. (10)]:

$$E_a = \frac{\left(\frac{D_{0,AH} + D_{0,BH} + \Delta_r H^\circ}{2}\right) (V_p - D_{0,AH} - D_{0,BH} + \Delta_r H^\circ)^2}{V_p^2 - (D_{0,AH} + D_{0,BH})^2 + \Delta_r H^{\circ 2}}, \quad (10)$$

for  $-4E_a^0 < \Delta_r H^\circ < 4E_a^0$

where  $\Delta_r H^\circ$  is the standard reaction enthalpy,  $D_{0,AH(BH)}$  is the bond dissociation enthalpy for AH (BH), and  $E_a^0$  is the intrinsic barrier, that is, the activation energy for  $\Delta_r H^\circ = 0$ . For very exothermic or very endothermic reactions, there is no classical transition state. The intrinsic barrier,  $E_a^0$ , depends on several generally unknown parameters, such as the parameters of the Pauli interaction potential, and can be treated as a fitting parameter.  $V_p$  is a parameter related to the intrinsic barrier and to the bond dissociation enthalpies [Eq. (11)]:

$$V_p = (D_{0,AH} + D_{0,BH}) \frac{(D_{0,AH} + D_{0,BH} + 2E_a^0)}{(D_{0,AH} + D_{0,BH} - 2E_a^0)} \quad (12)$$

Equation (10) is rather insensitive to the value of the average bond dissociation energy,  $(D_{0,AH} + D_{0,BH})/2$ . For the curve in Figure 4 the average bond dissociation energy was fixed at 400  $\text{kJ mol}^{-1}$ , a typical value for C–H bonds. Varying the average bond dissociation energy between 350 and 450  $\text{kJ mol}^{-1}$  changes the predicted activation energies by less than 0.2  $\text{kJ mol}^{-1}$  for the range of reaction enthalpies considered in Figure 4. The intrinsic barrier  $E_a^0$  was treated as an adjustable parameter and an optimized value of  $64.0 \pm 1.7 \text{ kJ mol}^{-1}$  was determined. Note that the ab initio value for the intrinsic barrier is 71.0  $\text{kJ mol}^{-1}$  (reaction (2) in Table 2). Changing the intrinsic barrier to the ab initio value of 71.0  $\text{kJ mol}^{-1}$  increases the predicted activation energies by 5 to 7  $\text{kJ mol}^{-1}$ . Since Equation (10) varies only with the standard reaction enthalpy, the barrier for hydrogen abstractions involving methyl radicals is almost exclusively determined by the relative stability of the reactant and product radicals.

The standard activation group additivity values,  $\Delta GAV^\circ(C_i^{T5})$ , can now be derived from the activation energies in Table 2. The symmetric abstraction of a hydrogen atom from methane by a methyl radical is chosen as the reference reaction. This is the smallest reaction in the homologous set, and it would be possible to perform highly accurate quantum chemical calculations for the activation energy for this reaction or to use accurate experimental data. The standard activation group additivity values are obtained from Table 2 by taking the difference between the activation energy for the reaction in which the corresponding group occurs and the activation energy of the reference reaction. For example, the standard activation group additivity value  $\Delta GAV^\circ$  for the  $C_1^{T5}-(C_d)(C)_2$  group (i.e., for a tertiary allylic abstracting radical, Figures 1 and 2) is obtained from the difference between the activation energy for reverse reaction (8) and the activation energy for the reference reaction (2), that is,  $124.1 - 71.0 = 53.1 \text{ kJ mol}^{-1}$ . The standard activation group additivity values for  $C_2^{T5}-(C_d)(C)_2$  (i.e., for a reaction forming a tertiary allylic radical) is  $28.5 - 71.0 = -42.5 \text{ kJ mol}^{-1}$ . In this way one primary  $\Delta GAV^\circ$  can be obtained from every calculated activation energy, and the reactions in Table 2 are a minimal set to obtain all standard activation group additivity values. The resulting primary standard activation group additivity values for activation energies are given in Table 3. Primary standard activation group additivity values for Arrhenius activation energies at 298 and 1000 K can be obtained in a similar way. The standard activation group additivity values can now be used to calculate activation energies for hydrogen abstraction reactions not included in the ab initio database.

### 3.3. Validation and Application of the Group Contribution Method

In this section, the accuracy of the group contribution method is discussed and its use is illustrated. For example, the activation energy for the abstraction of a tertiary hydrogen atom by a primary vinyl radical:

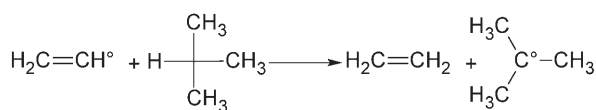
**Table 3.** Standard activation group additivity values and activation energy of the reference reaction [ $\text{kJ mol}^{-1}$ ] for the group contribution method for hydrogen abstraction activation energies,  $\Delta E^\ddagger(0\text{ K})$ . Reference reaction:



Activation energy of the reference reaction: 71.0

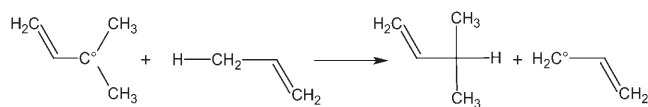
Group <sup>[a]</sup>	$\Delta\text{GAV}^\circ(\text{C}_1^{\text{T5}})$	$\Delta\text{GAV}^\circ(\text{C}_2^{\text{T5}})$
H	-15.0	-12.2
$\text{C}_r(\text{C})(\text{H})_2$	+4.2	-12.1
$\text{C}_r(\text{C})_2(\text{H})$	+5.7	-22.5
$\text{C}_r(\text{C})_3$	+2.9	-32.7
$\text{C}_r(\text{C}_d)(\text{H})_2$	+46.7	-28.2
$\text{C}_r(\text{C}_d)(\text{C})(\text{H})$	+52.4	-36.3
$\text{C}_r(\text{C}_d)(\text{C})_2$	+53.1	-42.5
$\text{C}_r(\text{C}_d)_2(\text{H})$	+83.2	-45.8
$\text{C}_r(\text{C}_d)_2(\text{C})$	+85.2	-50.3
$\text{C}_r(\text{C}_i)(\text{H})_2$	+33.4	-24.7
$\text{C}_r(\text{C}_i)(\text{C})(\text{H})$	+37.8	-33.7
$\text{C}_r(\text{C}_i)(\text{C})_2$	+39.7	-42.0
$\text{C}_r(\text{C}_t)_2(\text{H})$	+61.5	-43.9
$\text{C}_r(\text{C}_t)_2(\text{C})$	+65.2	-50.1
$\text{C}_r(\text{C}_B)(\text{H})_2$	+35.4	-24.5
$\text{C}_r(\text{C}_B)(\text{C})(\text{H})$	+39.6	-30.3
$\text{C}_r(\text{C}_B)(\text{C})_2$	+45.6	-34.0
$\text{C}_{id}^\circ(\text{H})$	-23.8	-1.7
$\text{C}_{id}^\circ(\text{C})$	-20.6	-11.6
$\text{C}_{id}^\circ(\text{C}_d)$	+9.1	-11.9
$\text{C}_{id}^\circ(\text{C}_t)$	-2.0	-22.4
$\text{C}_{it}$	-71.0	+44.6
$\text{C}_{iB}$	-36.3	+3.5
$\text{C}_{i,cyclo-6}^\circ(\text{H})$	+2.0	-23.2
$\text{C}_{i,cyclo-6}^\circ(\text{C})$	-0.5	-33.5
$\text{C}_{i,cyclo-5}^\circ(\text{H})$	+10.0	-26.8
$\text{C}_{i,cycloallylic}^\circ(\text{H})$	+51.4	-39.7

[a] C: alkylic carbon atom;  $\text{C}_d$ : double-bond carbon atom;  $\text{C}_t$ : triple-bond carbon atom; C<sup>°</sup>: radical carbon atom;  $\text{C}_B$ : carbon atom in a benzene ring;  $\text{C}_{cyclo-6}$ : alkylic carbon atom in a six-membered ring;  $\text{C}_{cyclo-5}$ : alkylic carbon atom in five-membered ring;  $\text{C}_{cycloallylic}$ : allylic carbon atom in a six-membered ring



involves the primary groups  $\text{C}_{1,d}^{\text{T5}}(\text{H})$  and  $\text{C}_2^{\text{T5}}(\text{C})_3$ . An activation energy of  $71.0 + (-23.8) + (-32.7) = 14.5 \text{ kJ mol}^{-1}$  is obtained with the data from Table 3. For comparison, the activation energy for this reaction was calculated with the ab initio CBS-QB3 method. The ab initio value of  $15.3 \text{ kJ mol}^{-1}$  is in agreement with the group contribution prediction.

The abstraction of a primary allylic hydrogen atom by a tertiary allylic radical was chosen as a second example:



The primary groups for this reaction are  $\text{C}_1^{\text{T5}}(\text{C})_2$  and  $\text{C}_2^{\text{T5}}(\text{C}_d)(\text{H})_2$  and the group contribution activation energy is  $71.0 + 53.1 + (-28.2) = 95.9 \text{ kJ mol}^{-1}$ . The CBS-QB3 ab initio value for this reaction is  $77.8 \text{ kJ mol}^{-1}$ , a difference of  $18.1 \text{ kJ mol}^{-1}$ .

This surprisingly large deviation led us to test the group contribution method for a larger set of reactions. Four characteristic radicals were included in the test set: hydrogen, isobutyl, primary allyl, and primary vinyl radicals. These radicals were selected for their distinctive nature as well as for their importance during hydrocarbon radical chemistry. Abstraction from 13 types of groups was considered: dihydrogen; primary, secondary, and tertiary alkylic, allylic, and propargylic; primary and secondary vinylic; and secondary vinylic/allylic. The barriers for the reverse reactions were also calculated. The activation energies  $\Delta E^\ddagger(0\text{ K})$  for all 88 reactions are presented in Table 4. The group contribution activation energies were also calculated for these reactions. The deviations with the ab initio values, that is, group contribution activation energy minus ab initio activation energy, are given in Table 5. Absolute deviations larger than  $10 \text{ kJ mol}^{-1}$  are written in boldface. Note that Table 5 is symmetric. It can be shown that the deviations in Table 5 are equal to the difference between the enthalpy of formation of the transition state predicted by the group additivity method [Eq. (5)] and the ab initio value, and are independent of the enthalpy of formation of the reactants. Therefore, the deviations are independent of the direction of the reaction. It can be concluded that the group contribution activation energies are rather accurate for hydrogen-transfer reactions involving hydrogen, alkylic hydrocarbons, and vinylic hydrocarbons, the largest deviations being less than  $6 \text{ kJ mol}^{-1}$ , and that Benson's group additivity method can be applied to the transition-state enthalpy of formation for these reactions [Eq. (4)].

Much larger deviations are found for reactions between allylic and propargylic hydrocarbons. In all cases, the group contribution method overestimates the activation energy. Clearly, Benson's group additivity method [Eq. (5)] does not hold for the transition-state enthalpy of formation of these reactions. To understand the origin of these deviations, the activation energies of Tables 2, 4, and 5 were plotted against the standard reaction enthalpies, together with the model of Blowers and Masel [Eq. (10)], by using the same intrinsic activation energy ( $E_a^0 = 64.0 \text{ kJ mol}^{-1}$ ) as for the previous set of reactions (see Figure 5). The same trend is again observed, but much larger deviations are found this time. The largest deviations are found toward lower activation energies, that is, the Blowers–Masel model also overestimates the activation energies, similar to the group contribution method. The deviations can be related to additional stabilization of the transition state relative to the transition state that is expected from reactions involving methyl radicals. We believe resonance effects cause these deviations. In the transition state, some stabilization by resonance occurs for all reactions involving an allylic or propargylic radical. The degree of resonance stabilization is, however, very different for the reactions between an allylic radical and methane—the reactions that were used to determine the  $\Delta\text{GAV}^\circ$ s—and the reactions involving two allylic radicals. The reactions

**Table 4.** Database of ab initio activation energies,  $\Delta E^\ddagger(0\text{ K})$  [ $\text{kJ mol}^{-1}$ ] for hydrogen abstraction reactions to test the validity of the group contribution method.

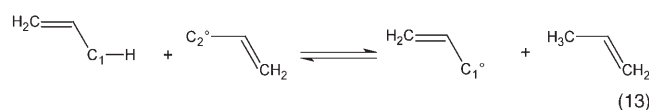
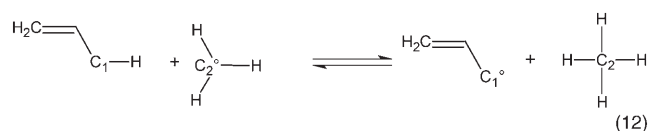
	H°												
H <sub>2</sub>	39.8	61.3	61.8	59.6	105.3	111.1	113.9	40.9	41.9	74.7	95.0	99.1	102.0
	42.3			61.0	101.6			34.9					
	30.9			48.6	88.7			24.2					
	21.2	41.6	41.2	37.6	75.4	80.3	79.2	15.3	15.5	45.2	61.3	64.7	66.0
	27.7	43.0	42.0	36.2	79.3	79.5	77.8	21.2	20.9	49.8	66.7	67.6	66.5
	19.8			27.3	65.7			11.2					
	15.5			19.1	57.0			5.9					
	60.2	73.3	74.5	73.0	118.2	122.0	123.7	44.5	47.7	76.3	102.5	107.3	110.1
	48.1			60.1	104.7			34.6					
	51.0			59.9	103.7			33.2					
	34.2			38.9	83.5			22.3					
	24.8			28.9	71.0			13.6					
	17.6			19.9	59.7			6.3					

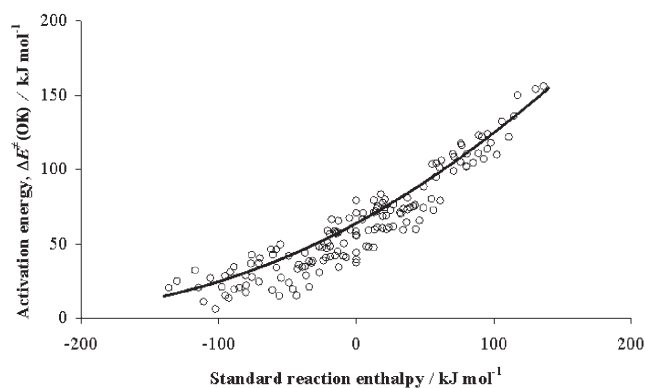
**Table 5.** Deviations between the ab initio activation energies,  $\Delta E^\ddagger(0\text{ K})$ , from Table 4 and the group contribution value (group contribution activation energy minus ab initio activation energy) [ $\text{kJ mol}^{-1}$ ]. Absolute deviations larger than  $10\text{ kJ mol}^{-1}$  are written in boldface.

	H°												
H <sub>2</sub>	4.0	1.7	2.7	2.1	0.1	0.0	-2.0	-5.9	-3.7	-6.9	-2.9	-2.5	-3.5
	1.7			0.8	4.1			0.2					
	2.7			2.8	6.5			0.5					
	2.1	0.8	2.8	3.6	9.6	<b>10.4</b>	<b>12.3</b>	-0.8	2.2	2.1	<b>10.3</b>	<b>11.3</b>	<b>12.0</b>
	0.1	4.1	6.5	9.6	<b>10.2</b>	<b>15.7</b>	<b>18.1</b>	-2.2	1.4	2.1	9.6	<b>13.0</b>	<b>16.0</b>
	0.0			<b>10.4</b>	<b>15.7</b>			-0.3					
	-2.0			<b>12.3</b>	<b>18.1</b>			-1.2					
	-5.9	0.2	0.5	-0.8	-2.2	-0.3	-1.2	1.1	1.0	2.1	0.2	-0.1	-1.1
	-3.7			2.2	1.4			1.0					
	-6.9			2.1	2.2			2.1					
	-2.9			<b>10.3</b>	9.6			0.2					
	-2.5			<b>11.3</b>	<b>13.0</b>			-0.1					
	-3.5			<b>12.0</b>	<b>16.0</b>			-1.1					

with methane are rather endothermic and the transition state is product-like. The radical electron is mostly located at the methyl species and little resonance stabilization occurs. Reactions involving two allylic radicals are nearly thermoneutral, and in the transition state both species have important radical character and are stabilized by resonance effects. This observation was verified by inspection of the Mulliken spin densities in the transition states of reactions (12) and (13):

Spin densities of 0.60 (C<sub>1</sub>) and 0.95 (C<sub>2</sub>) were calculated for the transition state of reaction (12). For reaction (13), the spin density at C<sub>1</sub> and C<sub>2</sub> amounts to 0.78, which indicates the



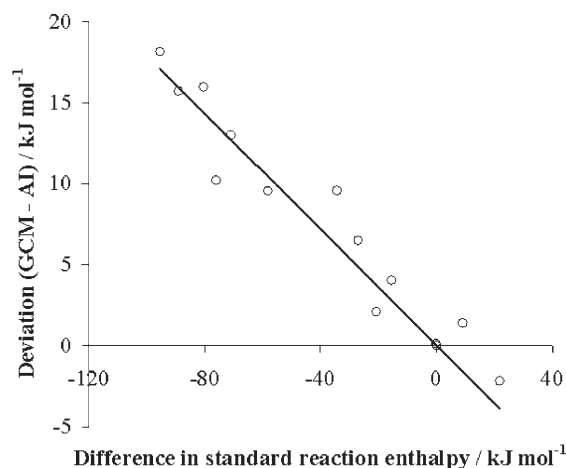


**Figure 5.** Evans–Polanyi plot for the hydrogen abstraction reactions from Table 4. The curve corresponds to the model of Blowers and Mase<sup>[28]</sup> [Eq. (10)] with a value of  $64.0 \text{ kJ mol}^{-1}$  for the intrinsic activation energy  $E_a^0$ .

higher radical character of both allylic carbon atoms in the transition state of this reaction. The difference in the location of the transition states also follows from a comparison of the transition-state geometries. For example, for reaction (12) the  $C_1$ –H distance at the transition state is 127 pm, and for reaction (13) it is 137 pm. Similar values are found for other reactions involving resonance-stabilized radicals. The group contribution method underestimates the resonance stabilization effect and therefore overestimates the activation energy for reactions between resonance-stabilized radicals.

At first sight, the introduction of additional standard activation group additivity values for  $H^{TS}-(C_1)(C_2)$  might account for these structural differences and might improve the group contribution method for these reactions. However, this approach would not improve the agreement for allylic radicals, since the same group  $H^{TS}-(C_1)(C_2)$  occurs for allylic and alkylic radicals. Additional  $\Delta GAV^\circ$ s would, however, be required for abstractions by hydrogen radicals,  $H^{TS}-(H)(C_2)$ , and by vinylic radicals,  $H^{TS}-(C_{1,d})(C_2)$ , for which the group contribution method gives satisfactory results. A better way to improve the group contribution method for hydrogen abstractions involving allylic and propargylic radicals is the introduction of an additional term to account for the resonance stabilization. The degree of resonance stabilization is related to the deviation of the transition-state geometry from the geometry of the methane + allylic/propargylic radical reaction and can be estimated from the reaction enthalpy. For reactions involving a resonance-stabilized radical, the stabilization increases when the transition state becomes more similar to the resonance-stabilized radical. Hence, for reactions involving a resonance-stabilized radical reactant, the stabilization increases when the reaction is more exothermic, and vice versa. This is illustrated in Figure 6, where the deviations between the group contribution activation energies and the ab initio values are plotted for the reactions involving a primary allylic radical as a function of the difference in reaction enthalpy between the studied reaction and the reaction involving methane. The correction term can be estimated by [Eq. (14)]

$$\Delta = 0.179 \cdot [\Delta_r H(298\text{K}) - \Delta_r H(298\text{K}; \text{methane})] \quad (14)$$



**Figure 6.** Deviations between activation energies,  $\Delta E^\ddagger(0 \text{ K})$ , obtained from the group contribution method (GCM) and ab initio values (AI) as a function of the difference in reaction enthalpy between the studied reaction and the reaction with methane for reactions involving a primary allylic radical.

where  $\Delta_r H(298 \text{ K})$  is the reaction enthalpy of the studied reaction and  $\Delta_r H(298 \text{ K}; \text{methane})$  is the reaction enthalpy for the reaction between the primary allyl radical and methane,  $+76.1 \text{ kJ mol}^{-1}$ . For reaction (13) the correction term amounts to  $0.179 (0.0 \text{ kJ mol}^{-1} - 76.1 \text{ kJ mol}^{-1}) = -13.6 \text{ kJ mol}^{-1}$ . From the data in Table 3 an activation energy of  $71.0 + 46.7 - 28.2 - 13.6 = 75.9 \text{ kJ mol}^{-1}$  is calculated, in reasonable agreement with the ab initio value of  $79.3 \text{ kJ mol}^{-1}$ . For the reaction between a tertiary allyl radical and propene, with an ab initio activation energy of  $77.8 \text{ kJ mol}^{-1}$ , the prediction improves even more: from  $95.9$  to  $78.8 \text{ kJ mol}^{-1}$ . Equation (14) can also be applied to reactions involving other resonance-stabilized radicals. For example, for the reaction between a tertiary butyl radical and 3-methyl-1-butyne, the group contribution method predicts an activation energy of  $31.9 \text{ kJ mol}^{-1}$ . After applying Equation (14), a value of  $25.6 \text{ kJ mol}^{-1}$  is obtained, which is in better agreement with the ab initio value of  $19.9 \text{ kJ mol}^{-1}$ . A more detailed study of reactions involving resonance-stabilized radicals is required to establish the accuracy of Equation (14) for determining the activation energy of reactions involving various types of resonance-stabilized radicals.

## 4. Conclusions

Hydrocarbon hydrogen abstraction reactions play an important role in many complex radical reaction networks. A kinetic database of accurate CBS-QB3 ab initio activation energies has been constructed for a set of 148 hydrogen abstraction reactions.

The group contribution method for activation energies<sup>[3]</sup> was extended to the family of hydrocarbon hydrogen abstraction reactions. The required standard activation group additivity values were derived from a minimal set of 57 high-level ab initio activation energies. The validity of the group contribution method was extensively tested by comparing group contribution activation energies with ab initio CBS-QB3 values. The

group contribution method yields accurate activation energies for hydrogen-transfer reactions between hydrogen, allylic hydrocarbons, and vinylic hydrocarbons. For reactions involving resonance-stabilized radicals, such as allyl and propargyl radicals, the transition state is believed to be stabilized by resonance effects and the group contribution method overestimates the activation energies, with deviations up to 18 kJ mol<sup>-1</sup>. A general correction factor to account for resonance stabilization effects in the transition state is proposed.

## Acknowledgements

M.S. is grateful to the Fund for Scientific Research-Flanders, Belgium (F.W.O.-Vlaanderen) for a research assistantship.

**Keywords:** ab initio calculations • abstraction reactions • hydrogen • radical reactions • thermodynamics

- [1] a) L. P. Hillewaert, J. L. Dierickx, G. F. Froment, *AIChE J.* **1988**, *34*, 17–24; b) S. Wauters, G. B. Marin, *Chem. Eng. J.* **2001**, *82*, 267–279; c) R. G. Susnow, A. M. Dean, W. H. Green, P. Peczak, L. J. Broadbelt, *J. Phys. Chem. A* **1997**, *101*, 3731–3740; d) W. H. Green, P. I. Barton, B. Bhattacharjee, D. M. Matheu, D. A. Schwer, J. Song, R. Sumathi, H.-H. Carstensen, A. M. Dean, J. M. Grenda, *Ind. Eng. Chem. Res.* **2001**, *40*, 5362–5370.
- [2] M. Saeys, M.-F. Reyniers, G. B. Marin, V. Van Speybroeck, M. Waroquier, *J. Phys. Chem. A* **2003**, *107*, 9147–9159.
- [3] M. Saeys, M.-F. Reyniers, G. B. Marin, V. Van Speybroeck, M. Waroquier, *AIChE J.* **2004**, *50*, 426–444.
- [4] a) S. W. Benson, *Thermochemical Kinetics*, 2nd ed., Wiley, New York, **1976**; b) N. Cohen, S. W. Benson, *Chem. Rev.* **1993**, *93*, 2419–2438.
- [5] J. Espinosa-Garcia, *J. Chem. Phys.* **2002**, *116*, 10664–10673.
- [6] J. Z. Pu, D. G. Truhlar, *J. Chem. Phys.* **2002**, *116*, 1468–1478.
- [7] a) R. Sumathi, H.-H. Carstensen, W. H. Green, Jr., *J. Phys. Chem. A* **2001**, *105*, 6910–6925; b) R. Sumathi, H.-H. Carstensen, W. H. Green, Jr., *J. Phys. Chem. A* **2001**, *105*, 8969–8984; c) R. Sumathi, H.-H. Carstensen, W. H. Green, Jr., *J. Phys. Chem. A* **2002**, *106*, 5474–5489.
- [8] M. L. Coote, *J. Phys. Chem. A* **2004**, *108*, 3865–3872.
- [9] M. T. Nguyen, S. Creve, L. G. Vanquickenborne, *J. Phys. Chem.* **1996**, *100*, 18422–18425.
- [10] Y. Kurosaki, T. Takayanagi, *J. Chem. Phys.* **1999**, *110*, 10830–10842.
- [11] H. Basch, S. Hoz, *J. Phys. Chem. A* **1997**, *101*, 4416–4431.
- [12] D. Z. Goodson, D. W. Roelse, W.-T. Chiang, S. M. Valone, J. D. Doll, *J. Am. Chem. Soc.* **2000**, *122*, 9189–9195.
- [13] a) B. S. Jursic, *J. Mol. Struct. (Theochem)* **1998**, *427*, 117–121; b) B. S. Jursic, *J. Mol. Struct. (Theochem)* **1998**, *430*, 17–22; c) B. S. Jursic, *J. Mol. Struct. (Theochem)* **1998**, *428*, 49–54.
- [14] S. W. Zhang, T. N. Truong, *J. Phys. Chem. A* **2003**, *107*, 1138–1147.
- [15] A. M. Mebel, K. Morokuma, M. C. Lin, *J. Chem. Phys.* **1995**, *103*, 3440–3449.
- [16] X. Zhang, Y. Ding, Z. Li, X. Huang, C. Sun, *J. Phys. Chem. A* **2000**, *104*, 8375–8381.
- [17] Y. Kurosaki, T. Takayanagi, *J. Chem. Phys.* **2000**, *113*, 4060–4072.
- [18] A. M. Mebel, M. C. Lin, T. Yu, K. Morokuma, *J. Phys. Chem. A* **1997**, *101*, 3189–3196.
- [19] I. V. Tokmakov, J. Park, S. Gheys, M. C. Lin, *J. Phys. Chem. A* **1999**, *103*, 3636–3645.
- [20] a) T. N. Truong, T.-T. Truong, *Chem. Phys. Lett.* **1999**, *314*, 529–533; b) T. N. Truong, *J. Chem. Phys.* **2000**, *113*, 4957–4964.
- [21] B. J. Lynch, D. G. Truhlar, *J. Phys. Chem. A* **2001**, *105*, 2936–2941.
- [22] J. K. Kang, C. B. Musgrave, *J. Chem. Phys.* **2001**, *115*, 11040–11051.
- [23] Y.-Y. Chuang, E. L. Coitiño, D. G. Truhlar, *J. Phys. Chem. A* **2000**, *104*, 446–450.
- [24] P. F. Su, L. C. Song, W. Wu, P. C. Hiberty, S. Shaik, *J. Am. Chem. Soc.* **2004**, *126*, 13539–13549.
- [25] a) N. M. Donahue, J. S. Clarke, J. G. Anderson, *J. Phys. Chem. A* **1998**, *102*, 3923–3933; b) N. M. Donahue, *J. Phys. Chem. A* **2001**, *105*, 1489–1497; c) J. S. Clarke, J. H. Kroll, N. M. Donahue, J. G. Anderson, *J. Phys. Chem. A* **1998**, *102*, 9847–9857; d) H. A. Rypkema, N. M. Donahue, J. G. Anderson, *J. Phys. Chem. A* **2001**, *105*, 1498–1506.
- [26] a) A. A. Zavitsas, *J. Am. Chem. Soc.* **1998**, *120*, 6578–6586; b) A. A. Zavitsas, *J. Phys. Chem. A* **2002**, *106*, 5041–5042.
- [27] X. Ma, H. H. Schobert, *Ind. Eng. Chem. Res.* **2003**, *42*, 1151–1161.
- [28] P. Blowers, R. Masel, *AIChE J.* **2000**, *46*, 2041–2052.
- [29] K. J. Laidler, *Chemical Kinetics*, 3rd ed., Harper Collins, New York, **1987**, p. 114.
- [30] C. Eckart, *Phys. Rev.* **1930**, *35*, 1303–1309.
- [31] a) M. L. Coote, M. A. Collins, L. Radom, *Mol. Phys.* **2003**, *101*, 1329–1338; b) G. A. Petersson, *Computational Thermochemistry* (Eds.: K. K. Irikura, D. Frurip), ACS Symposium Series, American Chemical Society, Washington, DC, **1998**, pp. 237–267.
- [32] J. P. A. Heuts, R. G. Gilbert, L. Radom, *J. Phys. Chem.* **1996**, *100*, 18997–19006.
- [33] a) V. Van Speybroeck, D. Van Neck, M. Waroquier, S. Wauters, M. Saeys, G. B. Marin, *J. Phys. Chem. A* **2000**, *104*, 10939–10950; b) V. Van Speybroeck, D. Van Neck, M. Waroquier, *J. Phys. Chem. A* **2002**, *106*, 8945–8950.
- [34] J. A. Montgomery, Jr., M. J. Frisch, J. W. Ochterski, G. A. Petersson, *J. Chem. Phys.* **2000**, *112*, 6532–6542.
- [35] G. A. Petersson, M. J. Frisch, *J. Phys. Chem. A* **2000**, *104*, 2183–2190.
- [36] Gaussian 98 (Revision A.7), M. J. Frisch, G. W. Trucks, H. B. Schlegel, G. E. Scuseria, M. A. Robb, J. R. Cheeseman, V. G. Zakrzewski, J. A. Montgomery, Jr., R. E. Stratmann, J. C. Burant, S. Dapprich, J. M. Millam, A. D. Daniels, K. N. Kudin, M. C. Strain, O. Farkas, J. Tomasi, V. Barone, M. Cossi, R. Cammi, B. Mennucci, C. Pomelli, C. Adamo, S. Clifford, J. Ochterski, G. A. Petersson, P. Y. Ayala, Q. Cui, K. Morokuma, D. K. Malick, A. D. Rabuck, K. Raghavachari, J. B. Foresman, J. Cioslowski, J. V. Ortiz, A. G. Baboul, B. B. Stefanov, G. Liu, A. Liashenko, P. Piskorz, I. Komaromi, R. Gomperts, R. L. Martin, D. J. Fox, T. Keith, M. A. Al-Laham, C. Y. Peng, A. Nanayakkara, C. Gonzalez, M. Challacombe, P. M. W. Gill, B. Johnson, W. Chen, M. W. Wong, J. L. Andres, C. Gonzalez, M. Head-Gordon, E. S. Replogle, J. A. Pople, Gaussian, Inc., Pittsburgh, PA, **1998**.
- [37] M. L. Coote, G. P. F. Wood, L. Radom, *J. Phys. Chem. A* **2003**, *107*, 12124–12138.
- [38] R. F. W. Bader, D. Bayles, *J. Phys. Chem. A* **2000**, *104*, 5579–5589.
- [39] *NIST Chemical Kinetics Database on the Web*, Public Beta Release 1.1, Standard Reference Database 17, Version 7.0. National Institute of Science and Technology, Gaithersburg, MD
- [40] K. J. Mintz, D. J. Le Roy, *Can. J. Chem.* **1978**, *56*, 941–949.
- [41] W. Tsang, *J. Phys. Chem. Ref. Data* **1988**, *17*, 887–952.
- [42] a) H.-X. Zhang, M. H. Back, *Int. J. Chem. Kinet.* **1990**, *22*, 21–35; b) S. I. Ahonkhai, M. H. Back, *Can. J. Chem.* **1988**, *66*, 578–583.
- [43] W. Tsang, R. F. Hampson, *J. Phys. Chem. Ref. Data* **1986**, *15*, 1087–1279.
- [44] D. L. Baulch, C. J. Cobos, R. A. Cox, C. Esser, P. Frank, T. Just, J. A. Kerr, M. J. Pilling, J. Troe, R. W. Walker, J. Warnatz, *J. Phys. Chem. Ref. Data* **1992**, *21*, 411–734.
- [45] P. M. Mayer, C. J. Parkinson, D. M. Smith, L. Radom, *J. Chem. Phys.* **1998**, *108*, 604–615.
- [46] a) M. G. Evans, M. Polanyi, *Proc. R. Soc. London Ser. A* **1936**, *154*, 133; b) J. C. Polanyi, *Acc. Chem. Res.* **1972**, *5*, 161–168.
- [47] W. Moller, E. Mozhukin, H. G. Wagner, *Ber. Bunsenges. Phys. Chem.* **1987**, *91*, 660–666.
- [48] Y. Hidaka, T. Oki, H. Kawano, *Int. J. Chem. Kinet.* **1989**, *21*, 689–695.

Received: April 14, 2005

Published online on December 2, 2005